

## Trisilanolphenyl-POSS nano-hybrid polyimide composite films: Miscibility and optical properties

Yan Zhang (张燕), Chenyu Guo, Xiao Wu, Jingang Liu\* (刘金刚)

School of Materials Science and Technology, China University of Geosciences, Beijing 100083, China  
(中国地质大学, 北京 100083)

E-mail: [liujg@cugb.edu.cn](mailto:liujg@cugb.edu.cn)

**Abstract:** Trisilanolphenyl-POSS (TSP-POSS) was physically blended with two poly(amic acid)s (PAAs) and one soluble polyimide (PI) with various adding proportions of 0, 5, 10, 15, 20, and 25wt% (TSP-POSS in total solids) in the current work. The main purpose of the work is to investigate the miscibility of TSP-POSS with the PAA or PI matrix so as to provide information for the future development of high performance PI films, such as low dielectric constant (low-*Dk*) films and so on. Two PAA matrices, including PAA-BP and PAA-PM were prepared from 3,3',4,4'-biphenyl- tetracarboxylic acid dianhydride (BPDA) and *para*-phenylenediamine (PDA) and pyromellitic anhydride (PMDA) and 4,4'-oxydianiline (ODA), respectively. The soluble PI matrix (PI-6F) was synthesized from 4,4'-(hexafluoroisopropylidene) diphthalic anhydride (6FDA) and 2,2-bis[4-(amino- phenoxy)phenyl]hexafluoropropane (BDAF). Experimental results indicated that PAA-PM showed good miscibility with the TSP-POSS filler even at the high loading of 25 wt%. Clear and homogeneous PI composite films with different TSP-POSS loadings (PI-PM-0~PI-PM-25) were successfully obtained by thermal imidization of the PAA-PM/TSP-POSS composite solutions. However, PAA-BP showed poor miscibility with the TSP-POSS additive. PI-BP/TSP-POSS composite films (PI-BP-0~PI-BP-25) obtained by thermally imidized at elevated temperatures showed opaque characteristics when the loading amount of TSP-POSS exceeded 10 wt%. All of the PI composite films based on PI-6F and TSP-POSS were optically transparent even at the high TSP-POSS loading of 25wt% and have the highest optical transmittance in the visible light region.

**Keywords:** polyimide, TSP-POSS, composite films, miscibility, optical properties

### 1. INTRODUCTION

Wholly aromatic polyimide (PI) films, known as poly(pyromellitic dianhydride-oxydianiline) (PI<sub>PMDA-ODA</sub>, with the trademark of Kapton<sup>®</sup> commercialized by Dupont in 1960s, USA), poly(biphenyl dianhydride-*p*-phenylenediamine) (PI<sub>BPDA-PDA</sub>, with the trademark of Upilex-S<sup>®</sup> commercialized by Ube in 1980s, Japan) and poly[(4,4'-(hexafluoroisopropylidene) diphthalic anhydride-2,2-bis

[4-(aminophenoxy)phenyl]hexafluoropropane)] (PI<sub>6FDA-BDAF</sub>, with the trademark of LaRC<sup>™</sup>-CP1<sup>®</sup> by Nexolve, USA) have been widely used in modern industry as high-performance protection or insulating components. In various applications, they usually exhibit outstanding properties, including high thermal stability, high dimensional stability at elevated temperatures, good environmental stability, and excellent dielectric properties. However, in some kinds of specific applications, the above mentioned pristine PI films somewhat showed shortcomings. In the past decades, the solution via combination with inorganic micro- or nanoparticles has been promising procedures in reducing the properties deterioration for common PI films using in such applications [1-4].

In the microelectronics industry, low dielectric constant (low-*Dk*) materials are crucially needed to increase the processing speeds of highly integrated circuits and reduce the parasitic capacitance, signal delays, crosstalk and power dissipation. It is well known that PI is widely used as a flexible circuit substrate in the microelectronics industry. However, most of aromatic PI films usually show high dielectric constant due to the formation of charge-transfer complexes (CTCs) between the diamine moiety and the dianhydride

unit where the former acts as an electron donor and the latter as an electron acceptor. The method for decreasing the dielectric constant of PI mainly includes incorporation of fluorine-containing groups, porous structures, or functional minerals [5-9]. In the above methods, polyhedral oligomeric silsesquioxane (POSS) additives have been paid much attention due to their nanostructured nature bridging the gap between ceramic (silicate) and organic materials. This concept is also suitable for the development of polymer composite films although the additives have to be elaborately designed so as to be well blended with the polymer film matrix at a molecular level [10-13]. Especially when the utilized POSS additive is soluble in the good solvents for poly(amic acid) (PAA) or soluble PI resins, homogeneous combination at a molecular level can usually be achieved between the PI matrix and the additives. During the past decades, several important reviews have been reported in the literature on the POSS/polymer nanocomposites, either focusing on the fire retardance features [14], polymer physics on segmental dynamics [15], or high-tech applications [16]. In our continuous efforts developing high-performance PI films for electrical and electronic applications, PI/inorganic nanoparticles composite films were always good candidates due to their good combined thermal and dielectric properties. However, good mechanical and optical properties are usually also desired in practical applications for such films.

In the current work, a series of POSS nano-hybrid PI composite films were prepared and the miscibility between the PI matrix and the POSS additive was investigated. The effects of incorporation of the POSS additives on the optical properties of the developed composite films were investigated in detail.

## 2. EXPERIMENTAL

### 2.1. Materials

Pyromellitic dianhydride (PMDA), 4,4'-oxydianiline (ODA), 3,3',4,4'-biphenyltetracarboxylic acid dianhydride (BPDA) and *para*-phenylenediamine (PDA) were purchased from Tokyo Chemical Industry Co., Ltd., Japan. 4,4'-(Hexafluoroisopropylidene) diphthalic anhydride (6FDA) and 2,2-bis[4-(aminophenoxy)phenyl]hexafluoropropane (BDAF) were purchased from Changzhou Sunlight Pharmaceutical Co. Ltd., China. The dianhydride monomers were dried in vacuo at 180°C for 12h prior to use and the diamine monomers were used directly. *N*-methyl-2-pyrrolidinone (NMP),  $\gamma$ -butyrolactone (GBL), and *N,N*-dimethylacetamide (DMAc) were purchased from Sigma-Aldrich and purified by distillation prior to use. Trisilanolphenyl-polyhedral oligomeric silsesquioxane (TSP-POSS) was purchased from Forsman co., Ltd., China and used as received. The other commercially available reagents were used without further purification.

### 2.2. Measurements

Attenuated total reflectance Fourier transform infrared (ATR-FTIR) spectrum was obtained on a Bruker Tensor-27 FT-IR spectrometer. Atomic force microscopy (AFM) was performed on a Bruker Multimode 8 AFM microscope with the tapping mode. Ultraviolet-visible (UV-Vis) spectra were recorded on a Hitachi U-3210 spectrophotometer at room temperature. The cutoff wavelength was defined as the point where the transmittance was zero in the spectrum. Prior to test, PI samples were dried at 100 °C for 1 h to remove the absorbed moisture. Yellow index (YI) and haze values of the PI films were measured using an X-rite color i7 spectrophotometer with PI film samples at a thickness of 20  $\mu$ m. The color parameters were calculated according to a CIE Lab equation.  $L^*$  is the lightness, where 100 means white and 0 implies black. A positive  $a^*$  means a red color, and a negative one indicates a green color. A positive  $b^*$  means a yellow color, and a negative one indicates a blue color.

### 2.3. PAA/TSP-POSS composite solution and PI/TSP-POSS composite films preparation

The preparation of PAA/TSP-POSS composite solution and film can be illustrated by the preparation of PAA-BP-5/TSP-POSS with PAA-BP as the matrix and TSP-POSS (5wt% loading) as the additive.

The unfilled PAA-BP solution was prepared according to the procedure described below. To a 1000-mL three-necked round-bottom flask equipped with a high-power electromagnetic stirrer, nitrogen inlet, and cold-water bath was added PDA (21.628 g, 200 mmol) and freshly-distilled DMAc (300 g). A clear diamine solution formed after stirring for 30 min under a nitrogen flow. Then, BPDA (58.844 g, 200 mmol) was added immediately, followed by additional DMAc (107 g) to adjust the solid content of the mixture to be 15 wt%. The mixture was stirred at room temperature for 24 h to afford a viscous solution, which was diluted to 10 wt% by adding additional DMAc solvent. The mixture was stirred for 1 h to obtain a homogeneous solution. After being purified by filtration through a 0.45- $\mu$ m Teflon syringe filter (Toyo Roshi Kaisha, Ltd., Japan), the obtained PAA solution was sealed and stored in a brown glass bottle filled with dry nitrogen in a refrigerator at -18 °C prior to use.

PAA-BP-5/TSP-POSS was prepared as follows. A 1000-mL three-necked flask equipped with a mechanical stirrer and a nitrogen inlet was charged with PDA (21.628 g, 200 mmol), TSP-POSS (4.235 g, 4.548 mmol) and DMAc (300 g). A clear solution formed after stirring for 30 min under a nitrogen flow. Then, BPDA (58.844 g, 200 mmol) was added immediately, followed by additional DMAc (129 g) to adjust the solid content of the mixture to be 15 wt%. The mixture was stirred at room temperature for 24 h to afford a viscous solution, which was diluted to 10 wt% by adding DMAc. The obtained PAA-BP-5/TSP-POSS solution was post-treated with the procedure as same as PAA-BP-0 mentioned above. The other PAA/TSP-POSS solutions with different POSS contents were synthesized with a similar route. PI-BP-5 film was prepared as follows. The stored PAA-BP-5/ TSP-POSS solution was warmed to room temperature and then spin-coated on a silicon wafer or quartz substrate (diameter: 50 mm, TKG Co., Ltd., Japan). The thickness was controlled by adjusting the spinning rate. The thickness of the specimens for the FT-IR and UV-Vis measurements was controlled to be 10  $\mu$ m and 20  $\mu$ m, respectively; and that of the specimens for thermal and mechanical property measurement was adjusted to 30–50  $\mu$ m. PI-BP-5/TSP-POSS film was obtained by thermally curing the PAA solution under nitrogen in an oven for 1h each at 80, 150, 250, and 300 °C, respectively. The obtained PI composite films were peeled off in deionized water and then dried in a heated air circulation drying oven at 120°C for 4h. The other PI films, including PI-BP-0, PI-BP-10, PI-BP-15, PI-BP-20, and PI-BP-25 were prepared according to a similar procedure.

The PAA-PM/TSP-POSS solution and PI-PM/TSP-POSS films were prepared in the same manner as PAA-BP/TSP-POSS and PI-BP/TSP-POSS, respectively.

#### **2.4. Soluble PI/TSP-POSS composite solution and films preparation**

Into a 1000 mL three-necked, round-bottomed flask equipped with a mechanical stirrer, a Dean-Stark trap and a nitrogen inlet, BDAF (51.8450 g, 100 mmol) was dissolved in GBL (150 g) to afford a clear solution. Then, 6FDA (44.4240 g, 100 mmol) was added in one batch and an additional volume of GBL (30 g) was to wash the residual dianhydride. After stirring 30min at room temperature, a pale-brown viscous solution was obtained and an exothermic reaction up to 60-70 °C was observed. Isoquinoline (0.5 g) and toluene (150 mL) was added as imidization catalyst and azeotropic agent, respectively. The reaction mixture was heated to 140°C in nitrogen and maintained for 6h. During the reaction, the toluene-water azeotrope was distilled out of the system and collected in the Dean-Stark trap. Then, the reaction mixture was continuously heated to 180 °C and maintain for 3h. After cooling to room temperature, the viscous PI-6F solution was carefully poured into an excess of ethanol to yield a silky white resin. The obtained white PI-6F resin was collected and dried at 80 °C in vacuum for 24 h.

PI resin prepared above was dissolved in newly distilled DMAc and various amounts of TSP-POSS (5wt%,

10wt%, 15wt%, 20wt% and 25wt% based on the total solid) dissolved in DMAc were added. The solid content of the final composite solution was maintained at 25 wt%. After the solution was mechanically mixed for 3h, the viscous PI composite solution was cast on clean and dust-free glass plates by a scraper, and then dried in a clean oven at 50°C(0.5h), 80°C(3h), 120°C(1h), 150°C(1h), 180°C(1h), 200°C(1h) and 250 °C(1h), respectively. The obtained PI composite films were peeled off in deionized water and then dried in a heated air circulation drying oven at 120°C for 4h.

### 3. RESULTS AND DISCUSSION

#### 3.1. PAA-BP/TSP-POSS composite solution and PI-BP/TSP-POSS composite films

A series of TSP-POSS blended biphenyl-type PAA and PI were synthesized from BPDA, PDA and various amounts of TSP-POSS additive. All the reaction mixtures maintained homogeneous during the PAA-BP/TSP preparation in DMAc solvent, indicating good miscibility of TSP-POSS and biphenyl PAA. Flexible and tough PI composite films were cast from the PAA solutions. It can be clearly seen that the optical transparency gradually deteriorate with the increasing loading of TSP-POSS in the composite films. When the addition proportion of TSP-POSS reached 10%, the films became opaque. This feature of the biphenyl series can be attributed to the poor miscibility of rigid-rod BPDA/PDA matrix and the TSP-POSS additive.

**Fig.1** presents the AFM images of PI-BP/TSP-POSS films. It can be clearly observed that the surface roughness of the films increased with the increasing loading of TSP-POSS additive. Obvious POSS aggregates were observed for PI-BP-25 sample and they dispersed into the PI matrix, forming the dispersed phase. This phase separation caused the opaque nature of the highly doped PI composite films. The specific optical properties will be discussed below.

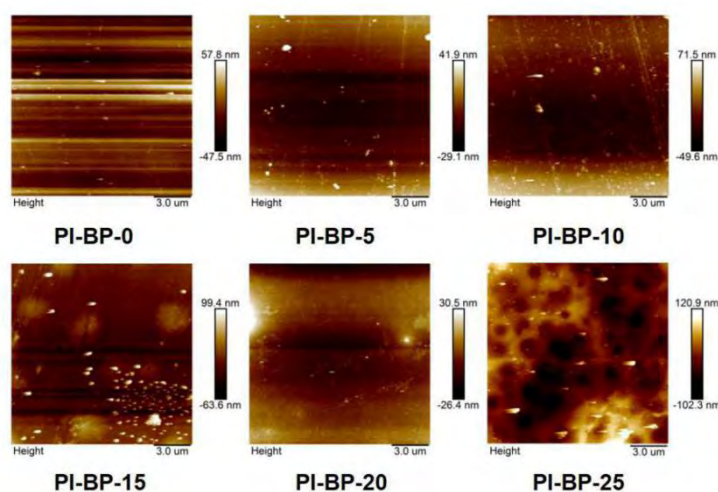


**Fig. 1.** AFM images of PI-BP/TSP-POSS composite films

The FT-IR spectra of the PI-BP films are illustrated in **Fig. 2**. The broad absorptions around 3312  $\text{cm}^{-1}$  due to the hydroxyl stretching vibrations of Si-OH in TSP-POSS disappeared in the spectra of the PI films. The characteristic absorptions of imide groups were observed at about 1782  $\text{cm}^{-1}$  ( $\nu_{\text{s,C=O}}$ ), 1719  $\text{cm}^{-1}$  ( $\nu_{\text{as,C=O}}$ ) and 1385  $\text{cm}^{-1}$  ( $\nu_{\text{as,C-N}}$ ), respectively. Meanwhile, the characteristic absorptions around 1132  $\text{cm}^{-1}$  ( $\nu_{\text{Si-O-Si}}$ ) were also detected in the FT-IR spectra of the PI films. These peaks indicated the successful combination of the PI matrix and TSP-POSS additives.

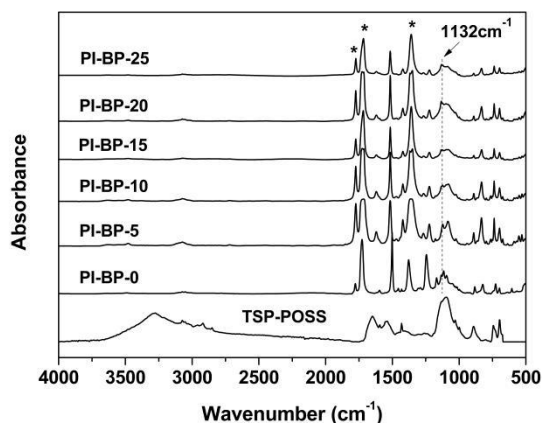


Fig. 2. FT-IR spectra of TSP-POSS and PI-BP/TSP-POSS composite films.

Generally speaking, the optical properties of the polymer composite films strongly depend on the dispersion effects of the additives in the polymeric matrices. For the current PI-BP/TSP-POSS system, TSP-POSS was physically blended into the PI-BP matrix. Although homogeneous molecular-level dispersion was achieved for the PAA precursors, apparent phase separation occurred for the PI systems. The optical properties of the PI-BP/TSP-POSS composite films were investigated by UV-Vis and yellow index measurements. **Fig. 3** exhibits the UV-Vis spectra of the PI-BP films at a thickness of 10  $\mu\text{m}$ . The cut off wavelengths, transmittances at 450 nm, and yellow indices of the films are summarized in **Table 1**. The optical parameters revealed the relationship between the compositions and the properties of the films. First, the transmittance of the films increased at a relatively lower amount of the POSS additive (<5 wt%). For instance, the  $T_{450}$  values of the films increased from 61.7% of PI-BP-0 to 72.2% of PI-BP-5; and the YI value decreased from 36.61 to 23.20 correspondingly. This is mainly due to the reduced molecular chains packing density caused by the bulky cage structure of the POSS additives. This is beneficial for the penetration of visible light. However, the transparency of the films rapidly fell with the further increase of the TSP-POSS loading amounts. PI-BP-20 and PI-BP-25 films were thoroughly opaque with the haze values of 100%. The opaque feature of the current PI composite films can mainly be attributed the phase separation of PI matrix and POSS additive, which could be deduced from the AFM measurements shown in **Fig. 1**.

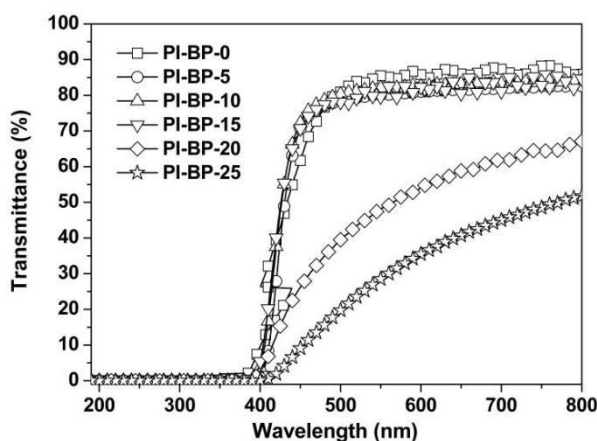


Fig. 3. UV-Vis spectra of PI-BP/TSP-POSS films.

**Table 1.** Optical properties of the PI-BP films.

	$\lambda^a$ (nm)	$T_{450}^a$ (%)	YI <sup>a</sup> ( $b^*$ )	haze (%)
PI-BP-0	382.5	61.7	36.61	0.72
PI-BP-5	380.5	72.2	23.20	0.71
PI-BP-10	385.5	70.7	40.39	20.88
PI-BP-15	387.0	70.6	46.83	20.99
PI-BP-20	392.5	26.2	46.33	100
PI-BP-25	399.5	9.1	42.44	100

<sup>a</sup> $\lambda$ : Cutoff wavelength;  $T_{450}$ : Transmittance at 450 nm; YI: yellow index.

### 3.2. PAA-PM/TSP-POSS composite solution and PI-PM/TSP-POSS composite films

A series of TSP-POSS blended PM-PAA solution and PM-PI films were synthesized from PMDA, ODA and various amounts of TSP-POSS additive. All the reaction mixtures maintained homogeneous during the PAA-PM/TSP-POSS preparation in DMAc solvent, indicating good miscibility of TSP-POSS and PAA. Flexible and tough PI composite films were cast from the PAA solutions. All the PI-PM/TSP-POSS composite films exhibited good optical transmittance in the visible light region.

**Fig. 4** presents the AFM images of PI-PM/TSP-POSS films. It can be clearly observed that the surface roughness of the films increased with the increasing loading of TSP-POSS additive. But when the adding proportion was over 15 wt%, the surface roughness decreased with the increasing loading of TSP-POSS additive. For instance, the surface roughness of PI-PM-25 film is lower than PI-PM-20 film. It may be due to the uniform dispersion of TSP-POSS in the PI matrix.

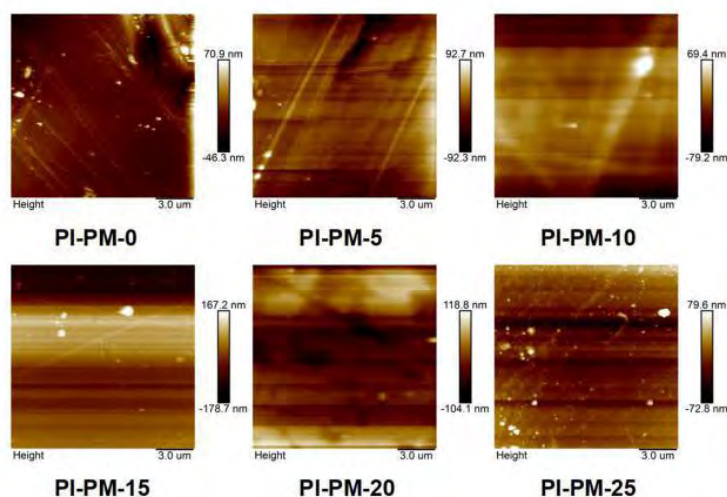


**Fig. 4.** AFM images of PI-PM/TSP-POSS composite films

The FT-IR spectra of the PI-PM films are illustrated in **Fig. 5**. The characteristic absorptions around 1135  $\text{cm}^{-1}$  ( $\nu_{\text{Si-O-Si}}$ ) were detected in the FT-IR spectra of the PI films. These peaks demonstrated the successful combination of the PI matrix and TSP-POSS additives.

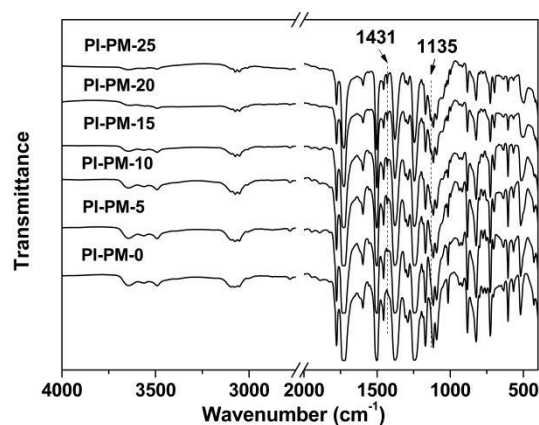


Fig. 5. FT-IR spectra of TSP-POSS and PI-PM/TSP-POSS composite films.

For PI-PM/TSP-POSS system, TSP-POSS was physically blended into the PI-PM matrix. Both the PAA and the PI achieved homogeneous molecular-level dispersion. The optical properties of the PI-PM/TSP-POSS composite films were investigated by UV-Vis and yellow index measurements. Fig.6 exhibits the UV-Vis spectra of the PI-PM films at a thickness of 10  $\mu\text{m}$ . The cut off wavelengths, transmittances at 450 nm, and yellow indices of the films are summarized in Table 2. The transmittance at 450nm increased with the increasing loading of TSP-POSS additive. This is also due attributed to the reduced molecular chains packing density caused by the bulky cage structure of the POSS additives. This is beneficial for the penetration of visible light. In addition, the YI value decreased from 81.62 to 64.70 at a relatively higher amount of the POSS additive (>15 wt%). The feature of the current PI composite films can mainly be attributed the good dispersion of PI matrix and POSS additive, which could be deduced from the AFM measurements shown in Fig.4.

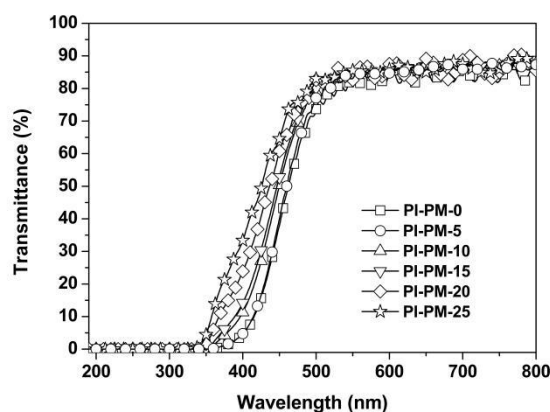


Fig. 6. UV-Vis spectra of PI-PM/TSP-POSS films.

Table 2. Optical properties of the PI-PM films.

	$\lambda^a$ (nm)	$T_{450}^a$ (%)	YI <sup>a</sup> ( $b^*$ )	haze (%)
PI-PM-0	355	37.9	79.41	0.66
PI-PM-5	353	40.0	74.52	0.70
PI-PM-10	353	50.4	76.73	0.80
PI-PM-15	354	52.7	81.62	0.99



PI-PM-20	352	60.8	70.45	1.13
PI-PM-25	352	64.6	64.70	1.57

<sup>a</sup>  $\lambda_c$ : Cutoff wavelength;  $T_{450}$ : Transmittance at 450 nm; YI: yellow index.

### 3.3. Soluble PI-6F/TSP-POSS composite films

TSP-POSS was dissolved in the soluble PI-6F resin in DMAc solvent. The obtained homogeneous PI solution indicated good miscibility of TSP-POSS and the soluble PI matrix. After curing at temperatures up to 250 °C, PI-6F/TSP-POSS composite films (PI-6F-0~PI-6F-25) were obtained. All the PI-6F/TSP-POSS composite films exhibited good optical transmittance in the visible light region.

**Fig. 7** presents the AFM images of PI-6F/TSP-POSS films. It can be clearly observed that the surface roughness of the films increased with the increasing loading of TSP-POSS additive. But when the adding proportion was over 20 wt%, the surface roughness decreased with the increasing loading of TSP-POSS additive. For instance, the PI-6F-25 film has a lower surface roughness than the PI-6F-20 film. It mainly attributed to the formation of continuous dispersion of TSP-POSS in the PI matrix.

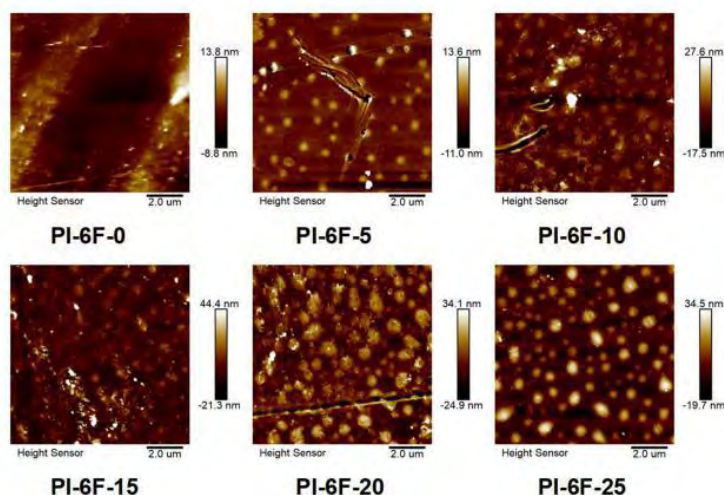


**Fig. 7.** AFM images of PI-6F/TSP-POSS composite films

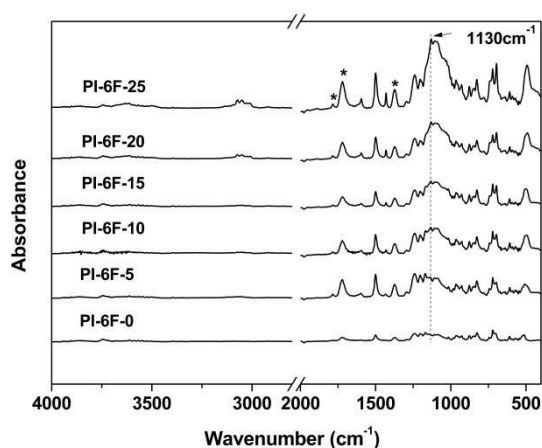


**Fig. 8.** ATR-FTIR spectra of TSP-POSS and PI-6F/TSP-POSS

The ATR-FTIR spectra of the PI-6F films are illustrated in **Fig. 8**. The characteristic absorptions of imide groups were observed at about 1784  $\text{cm}^{-1}$  ( $\nu_{s,\text{C=O}}$ ), 1720  $\text{cm}^{-1}$  ( $\nu_{as,\text{C=O}}$ ) and 1375  $\text{cm}^{-1}$  ( $\nu_{as,\text{C-N}}$ ), respectively.



Meanwhile, the characteristic absorptions around  $1130\text{ cm}^{-1}$  ( $\nu_{\text{Si-O-Si}}$ ) were also detected in the ATR-FTIR spectra of the PI films. These peaks indicated the successful combination of the PI matrix and TSP-POSS additives.

For the soluble PI-6F, TSP-POSS was physically blended into the PI matrix. Homogeneous dispersion at a molecular level was achieved for the PI systems. The optical properties of the PI-6F/TSP-POSS composite films were also investigated by UV-Vis and yellow index measurements. **Fig. 9** exhibits the UV-Vis spectra of the PI-6F films at a thickness of 25  $\mu\text{m}$ . The cut off wavelengths, transmittances at 450 nm, and yellow indices of the films are summarized in **Table 3**. The transmittance at 450 nm increased with the increasing loading of TSP-POSS additive. This is mainly due to the reduced molecular chains packing density caused by the bulky cage structure of the POSS additives. This is beneficial for the penetration of visible light. In addition, the excellent optical transparency was also due to the special chemical structure of resin. PIs derived from fluorine- containing 6FDA usually exhibit good solubility and low color due to the high electronegative nature of hexafluoroisopropylidene ( $>\text{C}(\text{CF}_3)_2$ ). This feature is beneficial for reducing the formation of CTCs and penetration of visible light; thus providing the PIs good optical transparency and low coloration.

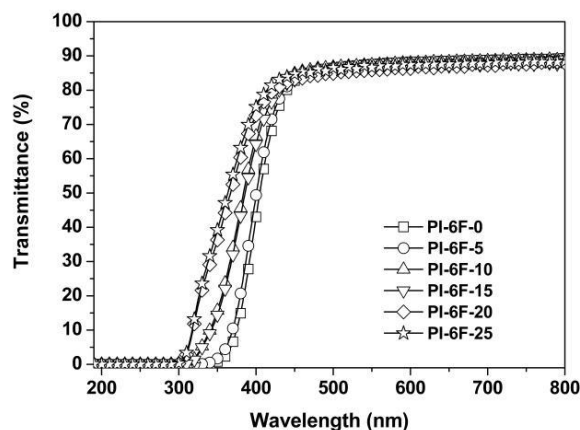


**Fig. 9.** UV-Vis spectra of PI-6F/TSP-POSS films.

**Table 3.** Optical properties of the PI-6F films.

	$\lambda^a$ (nm)	$T_{450}^a$ (%)	YI <sup>a</sup> ( $b^*$ )	haze (%)
PI-6F-0	347.5	82.8	4.40	2.05
PI-6F-5	316.0	83.1	5.71	9.48
PI-6F-10	302.5	83.2	5.78	3.27
PI-6F-15	339.0	83.3	6.28	4.70
PI-6F-20	315.5	84.8	3.83	2.44
PI-6F-25	301.5	84.7	3.80	5.14

<sup>a</sup> $\lambda$ : Cutoff wavelength;  $T_{450}$ : Transmittance at 450 nm; YI: yellow index.

#### 4. CONCLUSIONS

In the current work, TSP-POSS was utilized as the additive to be physically blended with three PI matrixes. A series of PI/POSS composite films were prepared and characterized. TSP-POSS exhibited poor miscibility with the PI-BP matrix when the addition proportion was higher than 10 wt%. Incorporation of TSP-POSS at high loadings deteriorated the optical transparency of the composite films. However,

TSP-POSS exhibited good miscibility with the PI-PM matrix even at the high POSS loading of 25wt%. As for the soluble PI matrix, TSP-POSS exhibited good miscibility with the PI-6F matrix. The derived PI-6F/TSP-POSS composite films exhibited excellent optical transparency.

### **Acknowledgement**

Financial support from the Fundamental Research Funds of China University of Geosciences, Beijing (No. 2652017345) is gratefully acknowledged.

### **References**

- [1] Song Z, Zhan H, Zhou Y. Polyimides: promising energy storage materials. *Angew Chem Inter Ed*, 2010, 49(45): 8444-8448.
- [2] Iredale R J, Ward C, Hamerton I. Modern advances in bismaleimide resin technology: A 21st century perspective on the chemistry of addition polyimides. *Prog Polym Sci*, 2017, 69: 1-21.
- [3] Liaw D J, Wang K L, Huang Y C, et al. Advanced polyimide materials: syntheses, physical properties and applications. *Prog Polym Sci*, 2012, 37(7): 907-974.
- [4] H.J. Ni, J.G. Liu, Z.H. Wang, S.Y. Yang, A review on colorless and optically transparent polyimide films: Chemistry, process and engineering applications. *J Ind Eng Chem*, 2015, 28: 16-27
- [5] Bae W J, Kovalev M K, Kalinina F, et al. Towards colorless polyimide/silica hybrids for flexible substrates. *Polymer*, 2016, 105: 124-132.
- [6] Song N, Shi K, Yu H, et al. Decreasing the dielectric constant and water uptake of co-polyimide films by introducing hydrophobic cross-linked networks. *Eur Polym J*, 2018, 101: 105-112.
- [7] Kowalczyk T C, Kosc T, Singer K D, et al. Loss mechanisms in polyimide waveguides. *J Appl Phy*, 1994, 76(4): 2505-2508.
- [8] Leu C M, Chang Y T, Wei K H. Polyimide-side-chain tethered polyhedral oligomeric silsesquioxane nanocomposites for low-dielectric film applications. *Chem Mater*, 2003, 15(19): 3721-3727.
- [9] Wahab M A, Mya K Y, He C. Synthesis, morphology, and properties of hydroxyl terminated POSS/polyimide low-k nanocomposite films. *J Polym Sci, Part A: Polym Chem*, 2008, 46(17): 5887-5896.
- [10] Vij V, Haddad T S, Yandek G R, et al. Synthesis of aromatic polyhedral oligomeric silsesquioxane (POSS) dianilines for use in high-temperature polyimides. *Silicon*, 2012, 4(4): 267-280.
- [11] Ayandele E, Sarkar B, Alexandridis P. Polyhedral oligomeric silsesquioxane (POSS)-containing polymer nanocomposites. *Nanomaterials*, 2012, 2(4): 445-475.[12]
- [12] Huang J, He C, Xiao Y, et al. Polyimide/POSS nanocomposites: interfacial interaction, thermal properties and mechanical properties. *Polymer*, 2003, 44(16): 4491-4499.
- [13] Verker R, Grossman E, Eliaz N. Effect of the POSS - Polyimide nanostructure on its mechanical and electrical properties. *Compo Sci Technol*, 2012, 72(12): 1408-1415.
- [14] Zhang W, Camino G, Yang R. Polymer/polyhedral oligomeric silsesquioxane (POSS) nanocomposites: An overview of fire retardance. *Prog Polym Sci*, 2017, 67: 77-125..
- [15] Raftopoulos K N, Pielichowski K. Segmental dynamics in hybrid polymer/POSS nanomaterials. *Progress in Kuo S W, Chang F C. POSS related polymer nanocomposites. Prog Polym Sci*, 2011, 36(12): 1649-1696.
- [16] Zhang X M, Liu J G, Yang S Y. A review on recent progress of R&D for high-temperature resistant polymer dielectrics and their applications in electrical and electronic insulation. *Rev Adv Mater Sci*, 2016, 46(1): 22-38.